Glucocorticoid Programming of the Fetal Male Hippocampal Epigenome

Ariann Crudo, Matthew Suderman, Vasilis G. Moisiadis, Sophie Petropoulos, Alisa Kostaki, Michael Hallett, Moshe Szyf, and Stephen G. Matthews

Department Pharmacology & Therapeutics (A.C., Ma.S., S.P., Mo.S.), Sackler Program for Epigenetics and Psychobiology (A.C., Ma.S., Mo.S.), and McGill Centre for Bioinformatics (Ma.S., M.H.) McGill University, Montreal, Quebec, Canada H3G1Y6; and Department of Physiology (V.M., A.K., S.G.M.), Departments of Obstetrics and Gynecology (S.G.M.), and Department of Medicine (S.G.M.), University of Toronto, Toronto, Ontario, Canada M5S 1A8

The late-gestation surge in fetal plasma cortisol is critical for maturation of fetal organ systems. As a result, synthetic glucocorticoids (sGCs) are administered to pregnant women at risk of delivering preterm. However, animal studies have shown that fetal exposure to sGC results in increased risk of behavioral, endocrine, and metabolic abnormalities in offspring. Here, we test the hypothesis that prenatal GC exposure resulting from the fetal cortisol surge or after sGC exposure results in promoter-specific epigenetic changes in the hippocampus. Fetal guinea pig hippocampi were collected before (gestational day [GD52]) and after (GD65) the fetal plasma cortisol surge (Term~GD67) and 24 hours after (GD52) and 14 days after (GD65) two repeat courses of maternal sGC (betamethasone) treatment (n = 3–4/gp). We identified extensive genome-wide alterations in promoter methylation in late fetal development (coincident with the fetal cortisol surge), whereby the majority of the affected promoters exhibited hypomethylation. Fetuses exposed to sGC in late gestation exhibited substantial differences in DNA methylation and histone h3 lysine 9 (H3K9) acetylation in specific gene promoters; 24 hours after the sGC treatment, the majority of genes affected were hypomethylated or hyperacetylated. However, 14 days after sGC exposure these differences did not persist, whereas other promoters became hypermethylated or hyperacetylated. These data support the hypothesis that the fetal GC surge is responsible, in part, for significant variations in genome-wide promoter methylation and that prenatal sGC treatment profoundly changes the epigenetic landscape, affecting both DNA methylation and H3K9 acetylation. This is important given the widespread use of sGC in the management of women in preterm labor. **(*Endocrinology* 154: 1168–1180, 2013)**

Endogenous glucocorticoids (GCs) are critical for fetal organ development including the lungs and brain. Synthetic GCs (sGCs) are administered to pregnant women at risk of delivering preterm, in order to mature lung function and to reduce respiratory distress syndrome after birth (1). However, sGC exposure in late gestation can alter normal brain growth and lead to permanent modifications in brain structure and function (2). The developing fetal brain contains high levels of GC receptor (GR) and mineralocorticoid receptor (MR) and therefore represents a primary target of sGCs (3–5). Evidence from animal studies indicates that maternally administered sGCs in late gestation can lead to lifelong changes in hypothalamic-pituitary-adrenal (HPA) axis function and behavior in adult offspring of numerous species including guinea pigs, mice, sheep, and nonhuman primates (6–9). More recent human studies have identified an increased risk of emotional and behavioral abnormalities in children exposed to elevated GC concentrations in utero by either antenatal sGC treatment or maternal stress (10, 11). The mechanism linking elevated GC levels with these abnormalities is currently unknown; however, substantial evidence has

ISSN Print 0013-7227 ISSN Online 1945-7170
Printed in U.S.A.

doi: 10.1210/en.2012-1980 Received September 25, 2012. Accepted January 4, 2013.
First Published Online February 6, 2013

Abbreviations: BETA, betamethasone; ChIP, chromatin immunoprecipitation; GC, glucocorticoid; GD, gestational day; GR, GC receptor; GRE, GC response element; H3K9, histone h3 lysine 9; HPA, hypothalamic-pituitary-adrenal; MeDIP, methylated DNA immunoprecipitation; MR, mineralocorticoid receptor; NT, no treatment; qChIP, quantitative ChIP; sGC, synthetic GC.

emerged indicating that epigenetic mechanisms play a role in the permanent reprogramming of the genome in response to early experiences and exposures (12–14). In fact, recent evidence has revealed that early nurturing experience can epigenetically reprogram the GR gene promoter in the hippocampus of rats (15) and humans (16).

Gene expression can be epigenetically modified through alterations in DNA methylation and histone chemical modifications such as histone acetylation (17) and methylation (18). DNA methylation in promoters and critical regulatory regions can suppress gene expression, whereas loss of DNA methylation in these regions is associated with gene activation (19, 20). Acetylation of the N-terminus of H3-histones at the K9 residue (21) is a global mark of gene activity. A bilateral relationship has been proposed for histone acetylation and DNA methylation (22). Methylated DNA attracts specific binding proteins that recruit chromatin-silencing complexes that contain histone deacetylases. The presence of deacetylases results in histone deacetylation (23). In addition, deacetylases in association with histone methyltransferases, can recruit DNA methyltransferases, thus linking chromatin silencing with DNA methylation (24, 25).

The guinea pig has been used extensively to investigate the long-term effects of prenatal GC exposure because the fetal pattern of brain development more closely resembles that of the human (26). Previous studies have shown that prenatal sGC exposure results in juvenile and adult guinea pig offspring that exhibit altered HPA function (27, 28), locomotor activity, and hippocampal neurotransmission (29). Most recently, effects on HPA function and behavior have been identified in second-generation offspring indicating multigenerational effects of prenatal sGC exposure (30). In addition, we have recently demonstrated that antenatal sGC treatment before the endogenous GC surge impacts the global DNA methylation state and associated methylation-related machinery in the fetus and neonate. Further, these effects are maintained into adulthood and are also evident in the second generation (31). Together, these studies indicate that prenatal sGC exposure results in long-term changes in the regulation of HPA function and behaviors and that these changes likely involve epigenetic processes.

Several studies from our laboratory have recently suggested that epigenetic reprogramming in DNA methylation, histone acetylation, and transcription in response to different environmental exposures early in life in humans and rodents is not limited to a small number of candidate genes but involves several gene networks and functional genomic pathways (32). The fact that we had observed global changes in DNA methylation in several tissues in the fetal and adult guinea pig in response to sGC supports the hypothesis that the changes in methylation in response to either a developmental surge in cortisol or sGC treatment involves numerous genes (31). In this study, we tested this hypothesis by delineating genome-wide promoter methylation and histone h3 lysine 9 (H3K9) acetylation landscapes in the fetal guinea pig hippocampus before and after the late gestation endogenous cortisol surge. The hippocampus was selected for this study due to the fact that it contains very high levels of corticosteroid receptors (MR and GR) and has been shown to be central in programming of HPA function and behaviors (2). We also determined how fetal exposure to sGC affected the epigenetic landscape of the hippocampus.

Materials and Methods

Female guinea pigs (Hartley strain, Charles River Canada, St Constant, Quebec, Canada) were housed and bred in our animal facility as previously described (33). All studies were performed according to protocols approved by the Animal Care Committee at the University of Toronto, in accordance with the Canadian Council for Animal Care.

Pregnant guinea pigs were injected sc with betamethasone (BETA; phosphate-acetate mix; Betaject, Sabex, Boucherville, Quebec, Canada; 1 mg kg-1) on gestational days (GD) 40, 41 (period of rapid neurogenesis), 50, and 51 (period of rapid brain growth) or received no treatment (control; no manipulation other than weighing, feeding, and changing of cage). In order to mimic the dose of sGC given to pregnant women in the management of preterm labor (~0.25 mg kg-1), a 4-fold higher dose was administered in the guinea pig (1 mg kg-1). This is necessary because the guinea pig GR has a 4-fold lower affinity for sGCs than the human GR (34, 35). Pregnant guinea pigs were euthanized on either GD52 (n = 3–4/gp; before the natural cortisol surge) or GD65 (n = 3–4/gp; after the cortisol surge), under anesthesia (isoflurane), by decapitation (Term~GD67). This generated four groups of pregnant guinea pigs; GD52NT (no treatment; NT), GD52BETA (BETA treated on GD40 and 41 and GD50 and 51), GD65NT (no treatment; NT), and GD65BETA (BETA treated on GD40 and 41 and GD50 and 51). Fetuses were removed and immediately decapitated to ensure no stress activation of cortisol. The hippocampus was dissected and frozen on dry ice. Guinea pigs deliver two to three offspring per litter. One male fetus was taken from each litter for subsequent analysis in order to prevent potential litter bias.

DNA and RNA extraction

Hippocampal DNA and RNA was extracted as previously described (31). DNA and RNA purity and concentrations were assessed using spectrophotometric analysis, and integrity was verified using gel electrophoresis.

Chromatin/DNA immunoprecipitation and microarray hybridization

The methylated DNA immunoprecipitation (MeDIP) (36) and the H3K9 acetylation chromatin immunoprecipitation

(ChIP) assays were adapted and performed as previously described (37, 38). The MeDIP assay was performed using an anti5-methylcytosine antibody (10 μg of antibody per 2 μg of DNA; Millipore Corp., Billerica, Massachusetts), and the H3K9 acetylation ChIP assay was performed with anti-acetyl-Histone (H3), lysine 9 (LYS9) antibody (10 μL of antibody per sample; Millipore), or normal rabbit IgG antibody (10 μg of antibody per sample; Santa Cruz Biotechnology, Santa Cruz, California). Amplification was undertaken using the Whole Genome Amplification kit (Sigma-Aldrich, St Louis, Missouri), labeling was performed with the CGH labeling kit (Invitrogen, Life Technologies, Carlsbad, California), and all the steps of hybridization, washing, and scanning were performed following the Agilent Technologies (Santa Clara, California) Mammalian ChIP-on-chip Protocol version 10.11 (39). DNA from three to four animals per group was used in the immunoprecipitation microarray experiments.

DNA methylation and H3K9 acetylation promoter microarrays

Labeled input and bound DNA samples were hybridized to a custom-designed 180K probe promoter tiling array (Agilent Technologies). Transcription start sites from 43 000 genes were obtained from the Ensembl gene annotation database (version 57.3; http://ensembl.org/) and tiled with probes from 1430 bp upstream to 350 bp downstream at 100 bp spacing. Agilent's Feature Extraction 9.5.3 Image Analysis Software was used to determine probe intensities from hybridization images, and the R software environment was used for statistical computing (40). Log-ratios of the bound (Cy5) to input (Cy3) microarray intensities were determined for each microarray. These ratios were then normalized using quantile normalization (41) assuming identical overall distribution of measurement across all samples.

Differential methylation and H3K9 acetylation between groups of samples was determined in several stages to ensure both statistical significance and biological relevance, as described previously (42). Significance was determined using the Wilcoxon rank-sum test comparing *t*-statistics of the probes within the region against those of all the probes on the microarray and then adjusted to obtain false discovery rates for each region.

Heat maps were obtained for a given sample group comparison by selecting the 250 probes most significantly associated with the group variable. The normalized intensities of these probes were then converted to z-scores across all samples and mapped to colors ranging from green for negative z-scores (hypomethylation and hypoacetylation) to red for positive z-scores (hypermethylation and hyperacetylation). Samples and probes were clustered using the Ward clustering algorithm with correlation as the distance metric. Significances of overlaps between lists of differentially methylated or acetylated gene promoters was derived using Fisher's exact test.

Sodium bisulfite mapping of DNA methylation

In order to validate the microarray data, sodium bisulfite mapping was performed as previously described (43). Genes with the largest significant methylation fold-change were selected for validation. Briefly, after bisulfite conversion, gene-specific PCR amplification of sodium bisulfite-treated DNA was performed for each animal. The primers used for bisulfite mapping do not contain any CG dinucleotide sequences to ensure that methylated and unmethylated sequences were amplified with equal efficiency. DNA (4 μg) was utilized for cloning using the TOPO TA cloning kit (Invitrogen, Life Technologies) as per manufacturers' recommendation. DNA, vector, and salt mixture were added to competent cells and incubated on ice (30 min). Cells were then heat shocked (30 s, 42°C) and immediately placed on ice (2 min). Super Optimal Broth with Catabolite repression medium (SOC; 300 μL) was added to competent cells and incubated (37°C, 45 min). Competent cells were then added to agar plates with ampicillin (0.1 g/L) and x-gal (40 mg/mL) and incubated overnight (37°C). Colonies were picked and grown in lysogeny broth overnight (37°C) on a shaker (225 rpm). Plasmid DNA was purified with High-Speed Plasmid Mini Kit (FroggaBio, Toronto, Ontario, Canada). Purified DNA from clones was sent to Genome Quebec facilities for automatic Sanger sequencing using the M13 reverse primer. Sodium bisulfite conversion quality was determined from sequencing results, confirming that C in non-CG sites was converted to T. DNA methylation was determined from the resulting sequencing at every single nucleotide. This was done by assigning a value of 1 to every methylated CG and a value of 0 to every unmethylated CG. Ten clones from three animals were sequenced from each group. Statistical analysis was undertaken using Prism (GraphPad Software, Inc, San Diego, California). The significance was set at $P < .05$. Enrichment in treatment compared with control was analyzed using unpaired *t*-tests.

Promoter regions of candidate genes were analyzed to determine presence of a GC response element (GRE). Positions of GREs were established based on consensus sequence. A match to at least one half of a GRE consensus sequence, AGAACANNNTGTTCT, was determined to be a GRE site.

Quantitative real-time PCR

Gene expression analysis was also undertaken in the genes that had been validated by bisulfite sequencing. Reverse transcription was performed using RNA (3 μg) as previously described (31). The primers used are presented in Supplemental Table 1 published on The Endocrine Society Journals' Online web site at http://endo.endojournals.org. Statistical analysis was undertaken using Prism (GraphPad Software, Inc). The significance was set at $P < .05$.

Quantitative ChIP (qChIP)

To validate the H3K9 acetylation ChIP microarrays, gene-specific real-time PCR was performed as previously described (31). Genes with the largest significant H3K9 acetylation fold-change were selected for validation. ChIP DNA was used for quantitative PCR. Bound and input DNA (50 ng) was used in all conditions. The relative concentrations were determined for bound and input samples based on standard curve (slopes were between −3.1 and −3.5). All samples were run in duplicate, and analysis of each gene was carried out in triplicate. The concentration of the amplified H3K9 acetylation over the concentration of the amplified input genomic DNA fraction was used to determine enrichment. Statistical analysis was undertaken using Prism (GraphPad Software, Inc). Enrichment in treatment compared with control was analyzed using unpaired *t*-tests. The significance was set at $P < .05$.

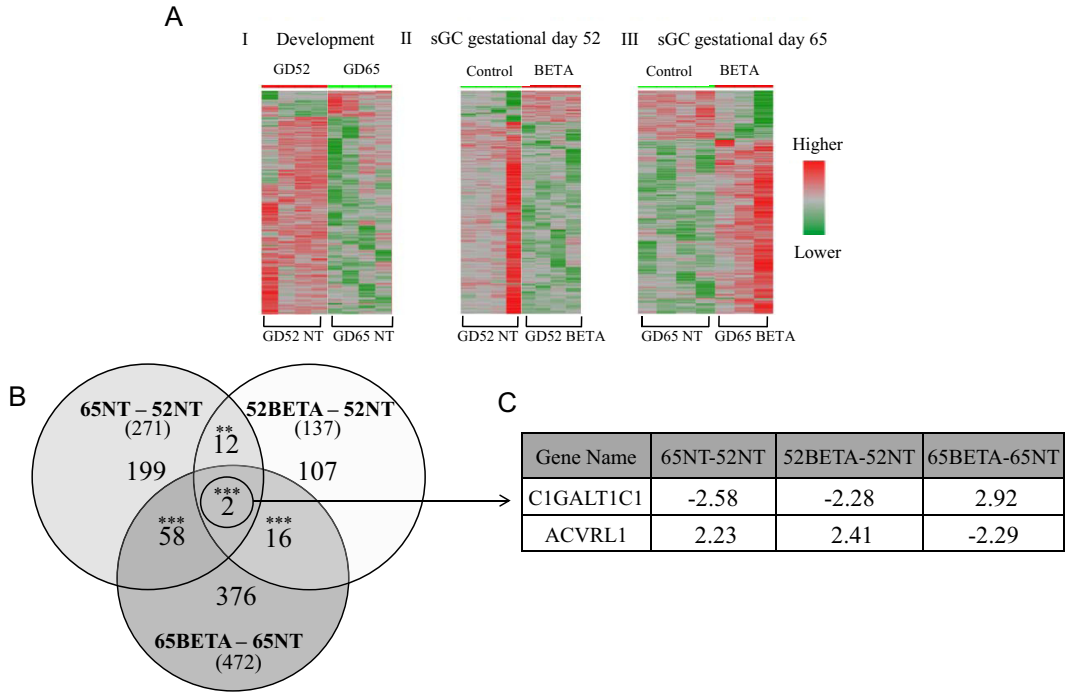

Gene Name	65NT-52NT	52BETA-52NT	65BETA-65NT
C1GALT1C1	-2.58	-2.28	2.92
ACVRL1	2.23	2.41	-2.29

Figure 1. Methylation Microarray Summary A, Heat map showing differential promoter DNA methylation in hippocampus after MeDIP microarray. Normalized signal intensities of probes (250) that significantly change following: I, fetal development (associated with the natural cortisol surge); II, the acute effect of sGC at GD52; and III, the longer-term effect of sGC at GD65. Each row represents one promoter, and each column represents an individual fetus. Red indicates higher signal and increased levels of DNA methylation whereas green indicates lower signal and lower methylation. B, A Venn diagram illustrating the number of genes that have significant differential methylation within each group and the number of significant genes that overlap between groups. The numbers in brackets indicate the total number of genes with differential methylation. C, The methylation profiles of the two genes that exhibited significant differential methylation in all three comparisons. The numbers represented in the table are the methylation fold-change values. A significant effect is represented as ** ($P < .01$) and *** ($P < .001$).

Results

GCs and alterations in genome-wide promoter DNA methylation

The promoter DNA methylation landscape before (GD52NT) and after (GD65NT) the endogenous GC surge is illustrated by the heat map in Figure 1A-I. Similar heat maps (Figure 1A, II and III) illustrate the effects of acute (GD52BETA vs GD52NT) and longer-term (GD65BETA vs GD65NT) effects of sGC exposure on promoter methylation. The rows of each heat map correspond to the 250 promoters in which methylation levels differentiate most strongly between the experimental groups. This analysis reveals a decrease in DNA methylation in a majority of the promoters that are different between GD52 and GD65 (endogenous cortisol surge) (Figure 1A-I) and after acute sGC treatment at GD52 (Figure 1A-II). However, the longer-term impact of sGCs in fetuses 14 days after exposure is increased methylation in most promoters relative to the normal methylation state (Figure 1A-III).

To characterize the methylation changes after GC exposure, we applied statistical tests to identify all significant differentially methylated promoters in all three comparisons. Significant methylation changes during normal development were identified in 271 gene promoters in the fetal hippocampus (Figure 1B; 65NT–52NT). With respect to fetal sGC exposure, at GD52 (24h after the final sGC injection), 137 gene promoters were differentially methylated compared with age-matched controls (Figure 1B; 52BETA–52NT). Interestingly, at GD65 (14 d after the final sGC injection) 472 gene promoters were differentially methylated compared with age-matched controls (Figure 1B; 65BETA-65NT). Supplemental Table 2 identifies the genes that overlap.

A number of the genes differentially methylated after the cortisol surge between GD52 and GD65 were also affected by sGC treatment, some showing differential methylation at GD52 and others showing long-term effects, at GD65. Of the 271 gene promoters that were differentially methylated between GD52 and GD65, 12 were also significantly affected by acute sGC exposure at GD52, whereas 58 were also affected at GD65, 14 days after sGC treatment (Figure 1B). Comparison of the genes affected by sGC at GD52 and GD65 revealed that only 16 genes were differentially methylated compared with controls at both time points (Figure 1B). In addition, the pro-

moters of two genes were significantly differentially methylated in all three groups ($P < .001$; Figure 1B). The methylation profiles of core 1 beta3-galactosyltransferase-specific molecular chaperone (*C1galt1c1*) and activin A receptor (*Acvrl1*) indicate that immediately after treatment, sGCs prematurely mature the methylation profile, mimicking development. However, as development progresses, the methylation profile of these genes becomes inverted (Figure 1C).

Validation of MeDIP microarrays with bisulfite sequencing

Methylation differences observed on the MeDIP microarrays were validated for MR (*Nr3C2*), baculoviral IAP repeat containing 2 (*Birc2*), E74-like factor 5 (*Elf5*), and ubiquitin protein ligase E3A (*Ube3a*) by bisulfite sequencing. Microarray data identified a decrease in methylation for both *Nr3c2* and *Birc2* in animals after the endogenous prepartum GC surge. Bisulfite sequencing of *Nr3c2* confirmed the observed decrease in methylation in GD65 animals, where CG site 2 contains a significant decrease (72%) in methylation ($P < .0001$; Figure 2A). *Birc2* showed one CG site with significant demethylation at GD65, which was accurately validated, indicating a significant decrease (73%) in methylation with advancing gestation ($P < .01$; Figure 2B). Microarray analysis revealed that at GD52, sGC-exposed animals showed hypermethylation in the *Elf5* gene promoter region. Bisulfite sequencing showed that in comparison to control, the GD52 sGC animals exhibited a consistent increase in methylation across four of five CG sites analyzed, with a significant increase at CG site 1 of 65% and CG site 2 of 45% ($P < .01$, $P < .01$; Figure 2C). The *Ube3a* gene promoter showed increased methylation in sGC-exposed animals at GD65. This hypermethylation state of *Ub3a* in GD65 sGC-treated animals was confirmed, showing a significant increase in methylation at CG site 2 (60%; $P < .01$; Figure 2D).

Impact of development and sGC on mRNA levels of candidate genes

In the fetal hippocampus, mRNA levels were determined for a number of candidate genes shown to have changes in promoter DNA methylation. With respect to normal development, hippocampal levels of *Nr3C2* and *Birc2* mRNA were significantly increased at GD65 compared with GD52 ($P < .0001$; Figure 3, A and B). These increases in gene expression corresponded to promoter hypomethylation (Figure 2, A and B). With respect to sGC treatment, at GD52, *Elf5* mRNA levels were significantly increased compared with controls ($P < .05$; Figure 3C), although this was associated with hypermethylation (Figure 2C). At GD65, sGC treatment resulted in a significant reduction in levels of hippocampal *Ube3a* mRNA compared with control ($P < .05$; Figure 3D), and this was associated with promoter hypermethylation (Figure 2D).

GCs and genome-wide promoter acetylation

Genome-wide landscapes of H3K9 acetylation associated with promoter regions were generated for hippocampi derived at GD52 and GD65. Our analysis did not detect a significant change in H3K9 promoter acetylation during normal development. We did, however, identify acute and longer-term effects of sGC exposure on promoter H3K9 acetylation that were highly significant (Figure 4). At GD52, sGC-exposed fetuses exhibited a broad change in histone acetylation with an effect on 1530 promoters. However, this difference was decreased by GD65 because only 393 promoters were differentially acetylated in the sGC-treated fetuses. Only 50 promoter differences were similar between the sGC groups at GD52 and GD65 (Figure 4B). As expected from this small overlap between the two time points, the functions of the genes also differed. For a comprehensive list of genes that overlap see Supplemental Table 3.

Validation of H3K9 ChIP microarrays with qChIP

H3K9 acetylation ChIP microarrays were validated by qChIP for zinc finger, AN1-type domain 6 (*Zfand6*), fibroblast growth factor 2_cavia porcellus (*Fgf2_Cavpo*), and ATPase type 13A3 (*Atp13a3*). An enrichment of H3K9 acetylation was detected by microarray analysis for both *Zfand6* and *Fgf_Cavpo* gene promoters in sGC-treated animals at GD52 (Figure 5, A and B). These results were confirmed through qChIP, which showed significant hyperacetylation for both genes ($P < .05$, $P < .001$; Figure 5, D and E). Microarray data indicated a hyperacetylation state for the gene promoter of *Atp13a3* in GD65 animals prenatally exposed to sGC (Figure 5C). These higher levels of acetylation were observed again through qChIP, illustrating a highly significant increase in acetylation in sGC-treated animals at GD65 ($P < .001$; Figure 5F).

The interaction of DNA methylation and histone acetylation

The impact of sGC exposure on the relationship between DNA methylation and H3K9 acetylation is illustrated in Figure 6. Previously, we have shown coordinated changes in DNA methylation and histone acetylation in response to maternal care (14). We therefore predicted that changes in DNA methylation and histone acetylation might target the same promoters. However, there is little overlap between the promoters that are differentially methylated and those that are differentially acetylated af-

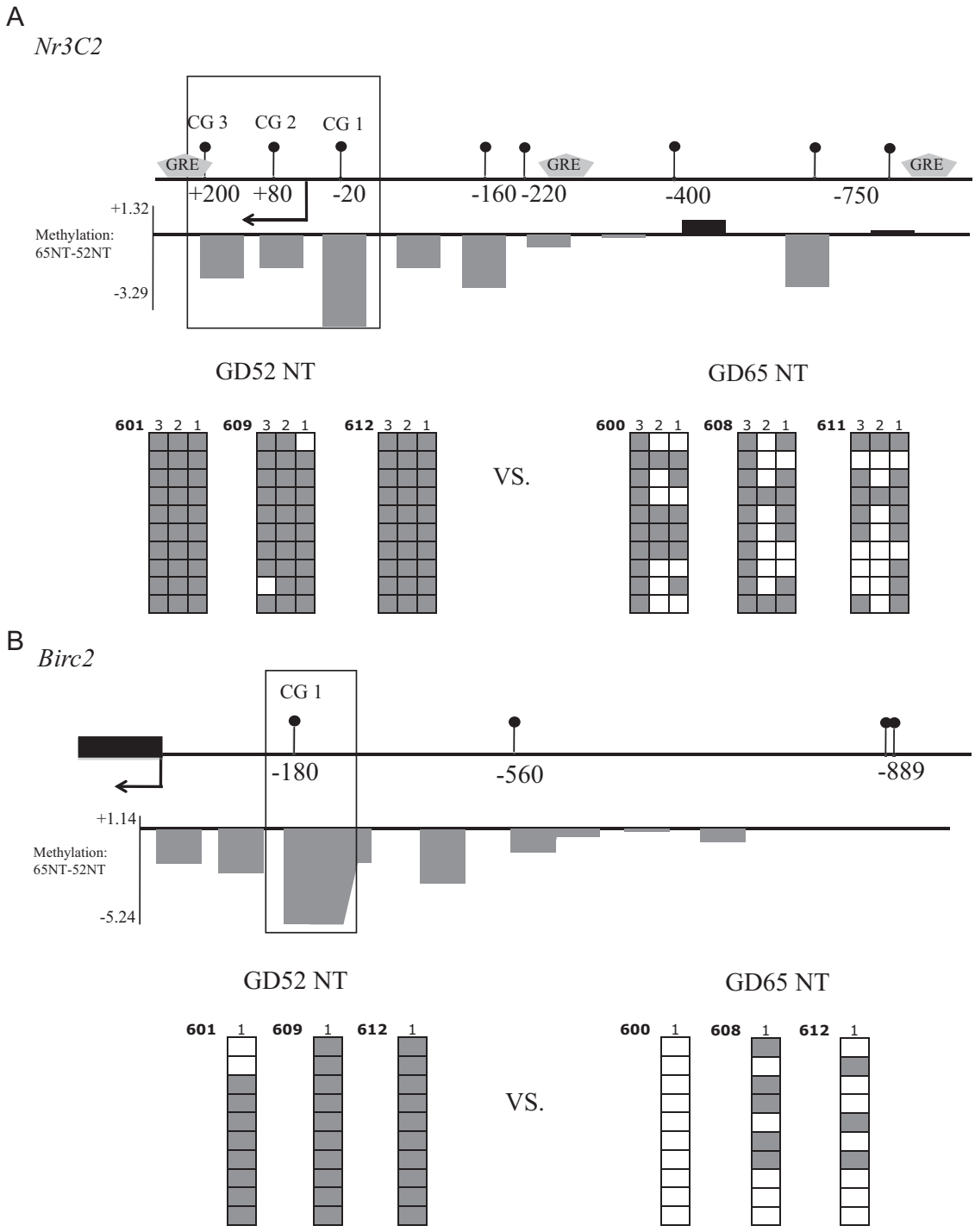

Figure 2. MeDIP Microarray Validation Methylation differences detected by microarray analysis for (A) *Nr3c2*, (B) *Birc2*, (C) *Elf5,* and (D) *Ube3a* were validated with bisulfite sequencing. 1) Schematic representation of the promoter region of each gene analyzed. CG sites are annotated relative to the transcription start site (TSS; indicated by arrow) of each gene, where each circle corresponds to one CG site. Predicted locations of GREs are also indicated. The observed tracks in the UCSC Genome Browser are shown, where the mean DNA methylation differences between different treatment groups are illustrated. Each bar represents a differently methylated region as shown by the microarray data. The black bars indicate mean increases in methylation, and gray bars correspond to decreases in methylation. The y-axis represents the methylation fold-change. 2) Bisulfite mapping analysis of sequences. Each grouping represents a different animal, with n = 3 per treatment group. Each column represents a CG dinucleotide, and each row represents an independent clone. A gray square represents a methylated CG dinucleotide, and a white square represents an unmethylated CG dinucleotide. The CG sites, depicted by a box, represent the sites analyzed in bisulfite sequencing.

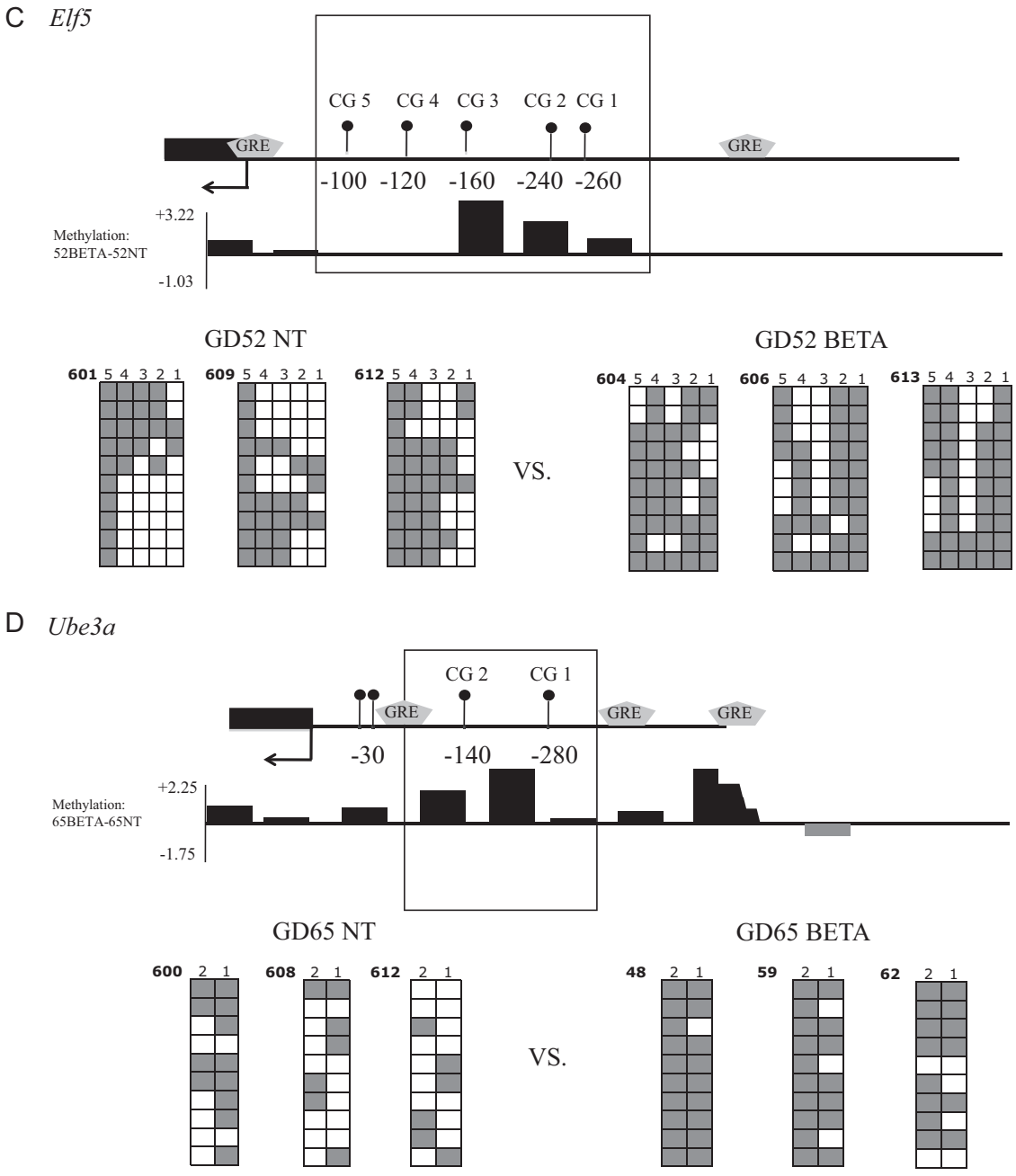

Figure 2. (Continued).

ter sGC treatment at either GD52 or GD65. At GD52, a single gene (thioredoxin reductase 3; *Trxr3*) exhibited a significant increase in both DNA methylation and H3K9 acetylation, whereas seven genes were significantly hypomethylated and hypoacetylated ($P < .05$; Figure 6A). By GD65, the significant interaction between differentially methylated and acetylated genes increased after sGC treatment, 17 gene promoters are both hypomethylated and hypoacetylated ($P < .001$; Figure 6B), and 31 gene promoters are both hypermethylated and hyperacetylated ($P < .001$; Figure 6B). For a comprehensive list of genes that overlap see Supplemental Table 4.

Discussion

Antenatal sGC treatment has been shown to have a widespread impact on physiologic function after birth and into adulthood (2, 28, 44). In this study, we used the guinea pig to determine whether the underlying mechanisms mediating the effects of antenatal sGC involve epigenetic modifications. Based on previous data from our laboratory, we reasoned that GCs would affect gene networks, and we therefore used a genome-wide approach to examine this question in the fetal hippocampus. By expanding our analysis beyond the candidate gene approach, and using high-

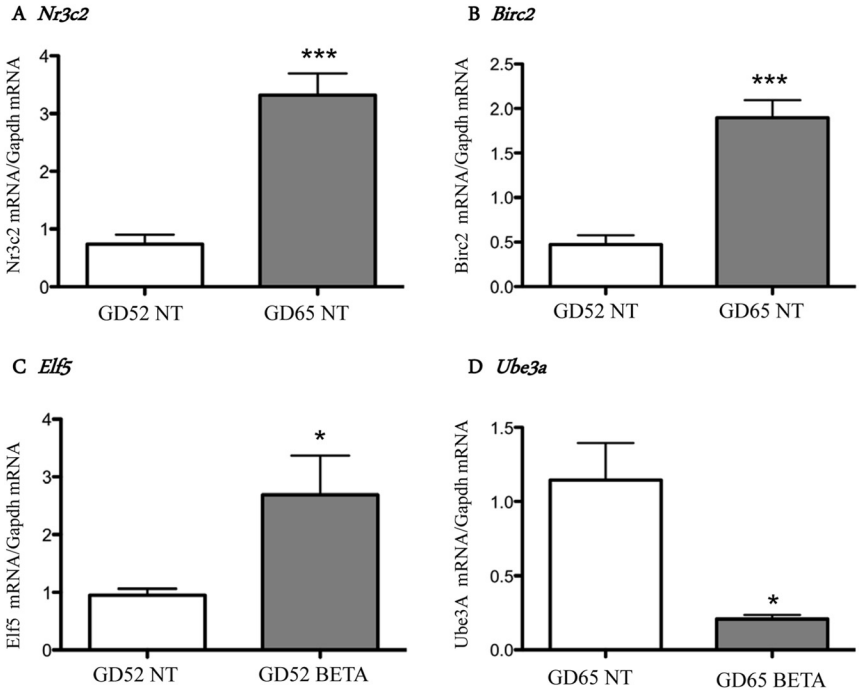

Figure 3. Expression Analysis of Candidate Genes with Differential Methylation Levels of mRNA were determined for genes validated to exhibit differential methylation. Hippocampal mRNA levels were determined for (A) *Nr3c2* and (B) *Birc2,* before (n = 3; open bars), and after (n = 3; solid bars) the endogenous cortisol surge. Hippocampal mRNA levels of were determined between sGC treatment (1 mg kg^{-1}; n = 3; solid bars) and nontreated controls (n = 3; open bars) at GD52 for (C) *Elf5* and at GD65 for (D) *Ube3a*. All mRNA expression is relative to the Gapdh reference gene (which did not change with treatment). Data are presented as mean ± SEM. A significant difference is represented as * ($P < .05$) and *** ($P < .001$).

density tiling microarrays, we were able to delineate modifications to the epigenetic landscape after the gestational GC surge, and antenatal sGC treatment. We have identified extensive genome-wide alterations in promoter DNA methylation in late fetal development (coincident with the fetal cortisol surge); most methylation changes involved hypomethylation or demethylation. No significant changes in H3K9 acetylation were observed during this stage of development. However, it is possible that there was inter-animal variation within the acetylation profiles that resulted in our inability to detect overall significant differences. Overall, these data are consistent with the hypothesis that GCs act as an essential signal or trigger for neurodevelopment (45) and suggest that the effects of GC exposure are mediated, in part, though mechanisms that include DNA methylation.

Previously, we have shown that with advancing gestation there were modifications in the global state of DNA methylation in several organ systems, including the brain (the cerebellum). Similar changes in methylation were observed after maternal sGC treatment. Further, changes in methylation were associated with altered expression of genes involved in methylation (31). One other study also correlated increased levels of fetal endogenous GCs with permanent demethylation of a key enhancer of the rat liver-specific tyrosine aminotransferase (*Tat*) gene (46). As a result of this demethylation, enhanced transcription factor binding was identified, which was observed long after the GC exposure (46). Thus, DNA demethylation served as a memory of the transient early exposure to GCs. In the present study, we have shown that fetuses exposed to sGC in late gestation exhibit substantial genome-wide differences in DNA methylation and H3K9 acetylation in specific gene promoters. Differential methylation and acetylation were observed in a number of genes as quickly as 24 hours after the final sGC treatment. Most genes affected became hypomethylated or hyperacetylated, which is consistent with genome activation. Further, more genes showed significant variation in methylation and acetylation 14 days after the final sGC treatment. Surprisingly, at GD65, 14 days after sGC exposure, these differences in methylation do not persist, but return to control levels, and a different set of promoters become hypermethylated or hypomethylated (Figure 1A-III). Similarly, the overall acetylation landscape is further modified, between 1 day and 14 days after sGC exposure (Figure 4A).

After sGC withdrawal, the impact on the epigenome remains and continues to modify the epigenetic landscape. This suggests that DNA methylation changes that are triggered by the transient exposure to sGC do not leave a permanent fixed memory in the epigenome as predicted by experiments with single-candidate genes (46), but rather launch a "dynamic" trajectory of changes in DNA methylation that evolve with time in the absence of further sGC exposure. Thus, the epigenome serves as a dynamic memory of early transient exposure to sGC rather than a static fixed change. In this connection, it is possible that the initial alterations in DNA methylation and chromatin modification trigger downstream changes in methylation in different genes. This could happen if some of the differentially methylated genes act as direct or indirect *trans*-acting regulators of methylation and chromatin modification of downstream genes. Feedback activity by these downstream target genes could, in turn, revert the state of methylation or chromatin modification of the upstream

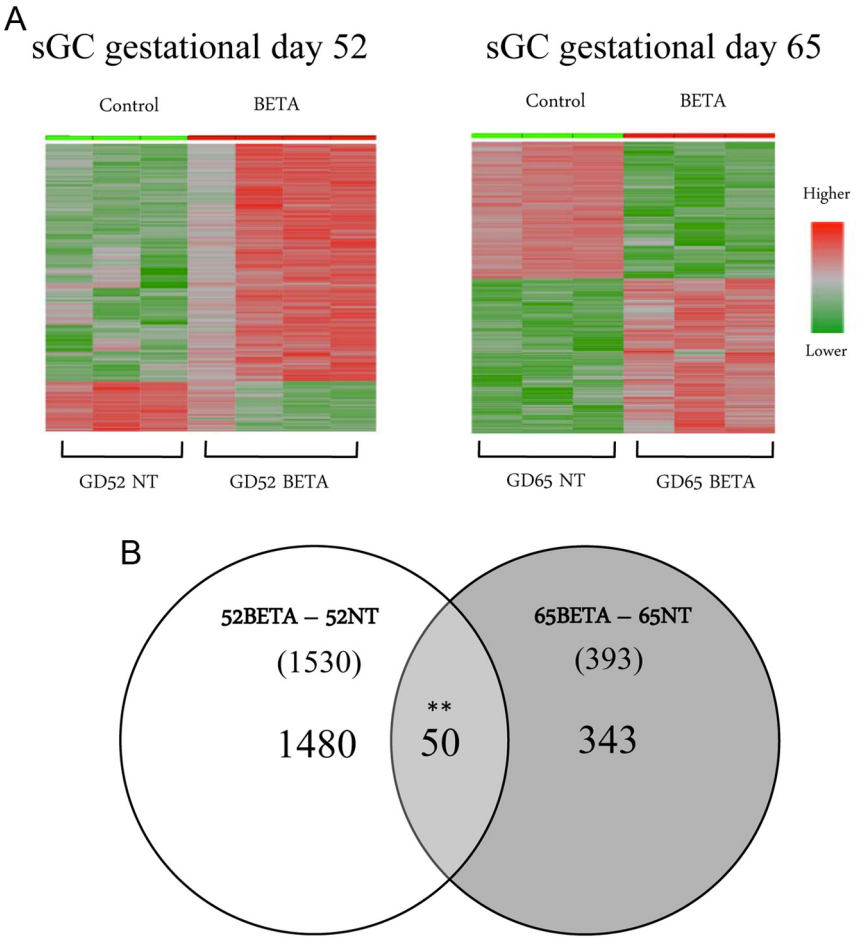

Figure 4. Acetylation Microarray Summary. A, Heat maps showing differential promoter acetylation after H3K9 ChIP microarray. Normalized signal intensities of probes (1000) that significantly differentiate between sample groups. The differentially acetylated sites were plotted to reveal the landscape of histone acetylation after exposure to sGC at GD52 and GD65. Each row represents one promoter, and each column represents an individual fetus. Red indicates higher signal and increased acetylation whereas green indicates lower acetylation. B, A Venn diagram illustrating the number of genes that have significant differential acetylation within each group and the number of significant genes that overlap between groups. The numbers in brackets indicate the total number of genes with differential acetylation. A significant effect is represented as ** ($P < .01$).

genes. Unraveling the hierarchical relationships among the genes involved in this cascade will require future studies.

During pregnancy, circulating cortisol levels are 5- to 10-fold higher in the maternal plasma compared with the fetus (47). This gradient results from a relatively inactive fetal adrenal combined with the presence of 11β-hydroxysteroid dehydrogenase type 2 (*11β-HSD2*) in the placenta. *11β-HSD2* catalyzes the conversion of active cortisol to its inactive metabolite, cortisone (48). Previously, we have shown a significant decrease in placental *11β-HSD2* in late pregnancy in the guinea pig, resulting in increased transfer of maternal cortisol to the fetus (48). This occurs in parallel with an increase in fetal HPA activity, leading to the fetal GC surge (49, 50). This surge is associated with the maturation of several organ systems including the brain (1). Our present data support the possibility that these cortisol-induced developmental changes involve, at least in part, epigenetic mechanisms.

It is possible that the methylation changes observed in fetal development are being driven by other developmental mechanisms. For example, fetal thyroid hormone levels increase in late gestation. Although these increases in thyroid hormone have been linked to the endogenous GC surge, thyroid hormones are independently involved in maturation of the fetal brain, heart, lung, and digestive system (51–53). The specific role of the endogenous cortisol surge in the epigenetic changes identified in the present study could be tested in future studies by pharmacologically inhibiting the endogenous cortisol surge in late gestation.

Our analysis allowed us to compare the epigenomic impact of maturation in late gestation (coincident with the endogenous cortisol surge) with an earlier pharmacologic exposure to sGC. A simplistic model would predict that sGC exposure might mimic the natural endogenous cortisol surge and precociously alter the developing epigenome. This fundamental model underlies the use of sGC treatment to promote fetal lung development in preterm infants. However, it must also be acknowledged that there are significant differences between the actions of cortisol and sGC. For example, cortisol binds to both GR and MR whereas sGCs bind GR but not MR (54). sGC can also bind the pregnane-X-receptor (*PXR*) and may mediate effects via this route (55). The differences between the DNA methylation responses to sGC or endogenous cortisol may result from the fact that sGC exposure occurs at an earlier time point than endogenous cortisol and, as such, may act on a different epigenomic matrix. With respect to the longer-term effects of sGC (ie, at GD65) on the fetal hippocampal epigenome, it is also important to consider the possibility that earlier sGC exposure alters the subsequent endogenous fetal GC surge, or other endocrine systems such as the thyroid axis (53). Further studies are

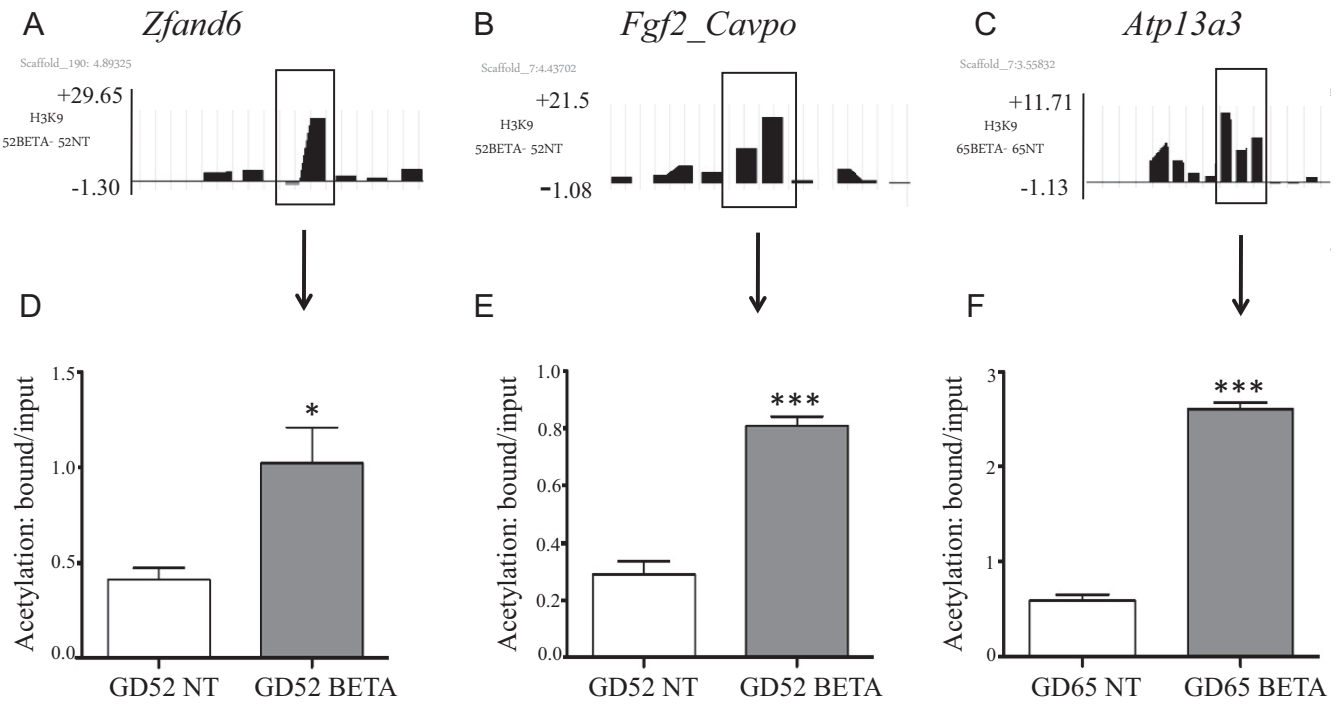

Figure 5. H3K9 ChIP Microarray Validation H3K9 acetylation differences detected by microarray analysis for *Zfand6*, *Fgf2_Cavpo*, and *ATP13A3* were validated by qChIP. A–C, The observed tracks in the UCSC Genome Browser, reveal gene location and mean H3K9 acetylation differences between different treatment groups. Each bar represents a differentially acetylated region as identified on the microarray. The y-axis represents the H3K9 acetylation fold-change values. Black bars indicate mean increases in acetylation, and gray bars correspond to decreases in acetylation. The region surrounded by a box represents the region that was amplified and validated with real-time PCR. D–F, Real-time PCR analysis of anti-H3K9-immunoprecipitated (bound fraction), normalized to the input samples. Levels of acetylation are shown in sGC-treated (n = 3; solid bars) and nontreated control (n = 3; open bars) animals. The y-axis represents acetylation enrichment. A significant difference between control and sGC-treated group is represented as * ($P < .05$) and *** ($P < .001$).

required to investigate these possibilities in the context of the developing epigenome.

In most, but not all, cases, histone acetylation and DNA methylation act in combination to affect gene expression (22). However, in the present study, no interaction between H3K9 acetylation and DNA methylation was observed. In response to sGCs, promoters undergo changes in either DNA methylation or H3K9 acetylation. This suggests that alternative strategies are utilized to affect different sets of genes, perhaps depending on the presence or absence of specific methyltransferases and/or deacetylases. In future experiments, it will be important to determine the mechanism underlying the relationship observed for DNA methylation and histone acetylation changes in response to sGCs. There are multiple forms of histone modifications, and therefore, sGC exposure may lead to other acetylation changes at sites such as H3K14, H4K5, or H4K12 (17). Further, it is important to note that, like all methods, microarray-based techniques have a number of limitations, such as: 1) The intensity of each probe only provides a weighted average of differential methylation and acetylation. 2) Methylation and acetylation are only measured within promoters. 3) Probe intensities provide relative measurements of methylation and acetylation, rather than absolute levels.

To further determine the implications of these epigenetic changes on gene expression, we examined the expression of the candidate genes validated for differential DNA methylation. Analysis of *Nr3c2* and *Birc2* mRNA revealed significant increases in expression with advancing development, which was inversely correlated with methylation. Further, *Ube3A* also revealed an inverse correlation between expression and methylation. However, expression analysis of *Elf5* identified a positive correlation between expression and methylation, whereby hypermethylation was associated with increased gene expression. Perhaps the site where methylation was observed in the promoter of *Elf5* acts as binding site for a repressor, and therefore, methylation of this site would prevent binding of the repressor, leading to an increase in expression. Overall, these data indicate that changes in the epigenome associated with development and sGC treatment are associated with altered levels of expression of a number of candidate genes. Further studies are required to determine the implications of sGC treatment on genome-wide gene expression.

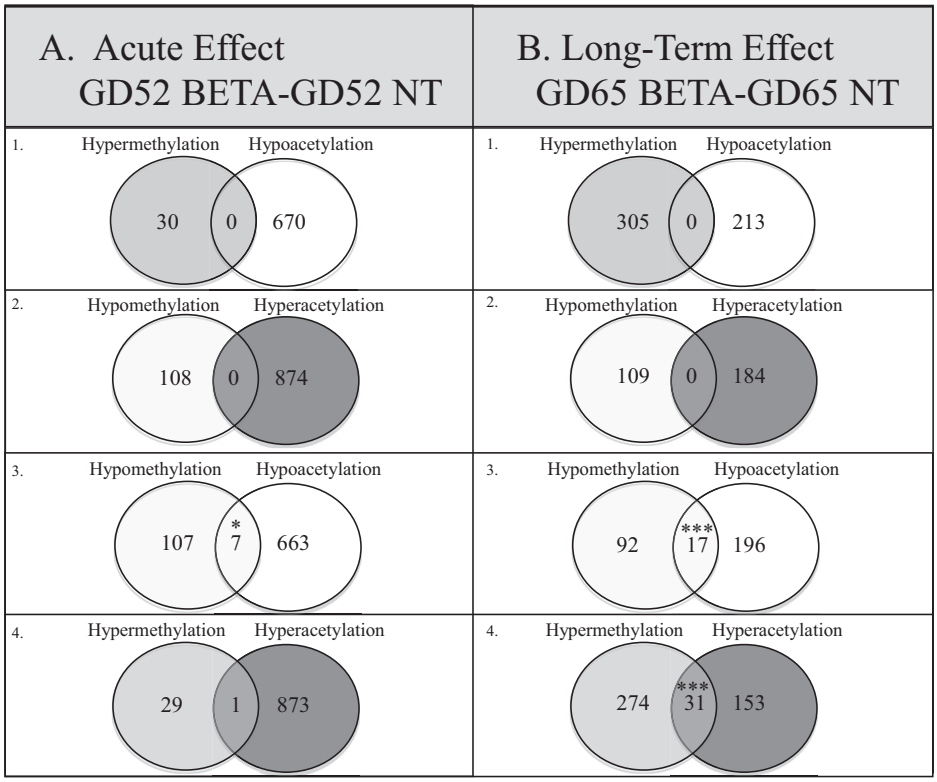

Figure 6. Interaction between Methylation and Acetylation Venn diagrams illustrating the overlap between the methylation and acetylation for acute effects of sGC at GD52 (panel A) and the long-term effect of sGC at GD65 (panel B). Venn diagrams are shown for the interaction between 1) hypermethylation and hypoacetylation; 2) hypomethylation and hyperacetylation; 3) hypomethylation and hypoacetylation; and 4) hypermethylation and hyperacetylation. A significant interaction is represented as * ($P < .05$) and *** ($P < .001$).

Bioinformatic analysis of the gene networks that were differentially methylated and acetylated in response to sGCs revealed that cardinal genes involved in nervous system, cardiovascular, and endocrine development are targeted (Supplemental Figures 1 and 2). It suggests that the functional roles of the genes affected are implicated in cardiovascular disease, hepatic system disease, and endocrine disorders that have been previously noted to be affected by sGCs in long-term follow-up studies (56–59). Antenatal sGC exposure has been shown to impact the development of cardiac noradrenergic and sympathetic processes and modify several metabolic processes in the heart (56–58, 60). Several studies have demonstrated that increased fetal GC exposure in late gestation is associated with adult hypertension, insulin resistance, type 2 diabetes, and cardiovascular disease (9, 59, 61). GCs are also known to play an important role in maturing the developing central nervous system, and prenatal sGC exposure has been shown to alter brain structure and synapse formation (62, 63). Determining the functional roles of the genes impacted by exposure to increased GCs in utero provides a means to understand the diverse phenotypes associated with antenatal sGC exposure.

In the present study, we have identified a large number of hippocampal gene promoters that undergo altered methylation and acetylation after sGC exposure. It is likely that some of these epigenetic changes underlie the altered physiologic function and behaviors identified in juvenile and adult offspring. For example, sGC exposure resulted in a 3.3-fold increase in methylation of the *GR* promoter at GD65; this may underlie long-term changes in regulation of HPA function. sGC treatment also had substantial acute effects on the methylation of several genes associated with synaptic transmission. For example, altered methylation was observed for 1) synaptotagmin 4 (*Syt4*), a gene involved in Ca^{2+}-dependent exocytosis of secretory vesicles (2.41-fold decrease); 2) reticulon 4 receptor (*Rtn4R*), a myelin-associated glycoprotein known to regulate axonal regeneration and plasticity in the adult central nervous system (4.06 fold-increase); and 3) leucine-rich repeat transmembrane neuronal 3 (*Lrrtm3*), a gene involved in nervous system development (2.97 fold-decrease). These differences may underlie the long-term changes in behavior and neurodendocrine function after antenatal sGC treatment.

GCs are known to alter gene expression in a number of ways. The most direct mechanism involves the binding of GCs to the GR or MR, which then undergo dimerization and translocation to the nucleus to directly interact with the GRE on the gene promoter (64). Alternatively, GCs

can act indirectly through the activation or repression of transcription factors, which regulate the expression of target genes (65). In this study, we observed, however, a broad epigenetic response: only a small number of genes affected are predicted to contain GREs (Supplemental Figure 3). This might indicate that GC exposure influences genes involved in gene networks or transcription factors, thus generating a much broader epigenetic response.

In conclusion, this study has shown, for the first time, that the endogenous GC surge in late gestation is associated with maturation of the fetal methylome. Our data suggest that the prepartum GC surge is responsible, in part, for developmental changes in genome-wide promoter methylation. Prenatal sGC exposure, before the GC surge, has a very profound effect on the epigenetic landscape, impacting both DNA methylation and H3K9 acetylation. However, it is now clear that the variations in promoter methylation and acetylation associated with sGC exposure are different from those identified during normal development (ie, after the natural GC surge). Further, profound effects of sGCs are evident on the fetal epigenome, up to 14 days after exposure. These data provide strong evidence that juvenile and adult metabolic, endocrine, and behavioral phenotypes associated with prenatal sGC treatment may be mediated, in part, by epigenetic mechanisms. This study has substantial relevance to clinical practice, because all pregnant women at risk of delivering preterm are treated with sGC in late gestation. Further studies are required to investigate the association of altered epigenetic state after sGC with the modified phenotype that occurs in juvenile and adult offspring that were prenatally exposed to sGC.

Acknowledgements

Address all correspondence and requests for reprints to: Stephen G. Matthews, Department of Physiology, Faculty of Medicine, University of Toronto, 1 King's College Circle, Toronto, Ontario, Canada M5S 1A8. E-mail: Stephen.Matthews@utoronto.ca.

This work was supported by Grant MOP-97736 from the Canadian Institute of Health Research (to S.G.M. and Mo.S.) Mo.S. is a fellow of the Canadian Institute for Advanced Research and is supported by a GlaxoSmithKline/Canadian Institutes of Health Research professorship in pharmacology.

Disclosure Summary: There is no conflict of interest to report that prejudices the impartiality of this research.

References

1. **Liggins GC, Howie RN.** A controlled trial of antepartum glucocorticoid treatment for prevention of the respiratory distress syndrome in premature infants. *Pediatrics*. 1972;50:515–525.
2. **Kapoor A, Petropoulos S, Matthews SG.** Fetal programming of hypothalamic-pituitary-adrenal (HPA) axis function and behavior by synthetic glucocorticoids. *Brain Res Rev*. 2008;57:586–595.
3. **Owen D, Matthews SG.** Glucocorticoids and sex-dependent development of brain glucocorticoid and mineralocorticoid receptors. *Endocrinology*. 2003;144:2775–2784.
4. **Owen D, Banjanin S, Gidrewicz D, McCabe L, Matthews SG.** Central regulation of the hypothalamic-pituitary-adrenal axis during fetal development in the Guinea-pig. *J Neuroendocrinol*. 2005;17:220–226.
5. **Andrews MH, Matthews SG.** Regulation of glucocorticoid receptor mRNA and heat shock protein 70 mRNA in the developing sheep brain. *Brain Res*. 2000;878:174–182.
6. **Sloboda DM, Moss TJ, Gurrin LC, Newnham JP, Challis JR.** The effect of prenatal betamethasone administration on postnatal ovine hypothalamic-pituitary-adrenal function. *J. Endocrinol*. 2002;172:71–81.
7. **Uno H, Eisele S, Sakai A, et al.** Neurotoxicity of glucocorticoids in the primate brain. *Horm Behav*. 1994;28:336–348.
8. **Liu L, Li A, Matthews SG.** Maternal glucocorticoid treatment programs HPA regulation in adult offspring: sex-specific effects. *Am J Physiol Endocrinol Metab*. 2001;280:E729–E739.
9. **Levitt NS, Lindsay RS, Holmes MC, Seckl JR.** Dexamethasone in the last week of pregnancy attenuates hippocampal glucocorticoid receptor gene expression and elevates blood pressure in the adult offspring in the rat. *Neuroendocrinology*. 1996;64:412–418.
10. **French NP, Hagan R, Evans SF, Mullan A, Newnham JP.** Repeated antenatal corticosteroids: effects on cerebral palsy and childhood behavior. *Am J Obstet Gynecol*. 2004;190:588–595.
11. **Glover V.** Annual research review: prenatal stress and the origins of psychopathology: an evolutionary perspective. *J Child Psychol Psychiatry*. 2011;52:356–367.
12. **Szyf M, Weaver IC, Champagne FA, Diorio J, Meaney MJ.** Maternal programming of steroid receptor expression and phenotype through DNA methylation in the rat. *Front Neuroendocrinol*. 2005;26:139–162.
13. **Weaver IC, Champagne FA, Brown SE, et al.** Reversal of maternal programming of stress responses in adult offspring through methyl supplementation: altering epigenetic marking later in life. *J Neurosci*. 2005;25:11045–11054.
14. **Weaver IC, Cervoni N, Champagne FA, et al.** 2004 Epigenetic programming by maternal behavior. Nat Neurosci 7:847–854.
15. **Weaver IC, Diorio J, Seckl JR, Szyf M, Meaney MJ.** Early environmental regulation of hippocampal glucocorticoid receptor gene expression: characterization of intracellular mediators and potential genomic target sites. *Ann NY Acad Sci*. 2004;1024:182–212.
16. **McGowan PO, Sasaki A, D'Alessio AC, et al.** Epigenetic regulation of the glucocorticoid receptor in human brain associates with childhood abuse. *Nat Neurosci*. 2009;12:342–348.
17. **Wade PA, Pruss D, Wolffe AP.** Histone acetylation: chromatin in action. *Trends Biochem Sci*. 1997;22:128–132.
18. **Jenuwein T.** Re-SET-ting heterochromatin by histone methyltransferases. *Trends Cell Biol*. 2001;11:266–273.
19. **Razin A, Riggs AD.** DNA methylation and gene function. *Science*. 1980;210:604–610.
20. **Razin A.** CpG methylation, chromatin structure and gene silencing-a three-way connection. *Embo J*. 1998;17:4905–4908.
21. **Perry M, Chalkley R.** Histone acetylation increases the solubility of chromatin and occurs sequentially over most of the chromatin. A novel model for the biological role of histone acetylation. *J Biol Chem*. 1982;257:7336–7347.
22. **D'Alessio AC, Szyf M.** Epigenetic tete-a-tete: the bilateral relationship between chromatin modifications and DNA methylation. *Biochem Cell Biol*. 2006;84:463–476.
23. **Nan X, Ng HH, Johnson CA, et al.** Transcriptional repression by the methyl-CpG-binding protein MeCP2 involves a histone deacetylase complex [see comments]. *Nature*. 1998;393:386–389.

24. **Fuks F, Burgers WA, Brehm A, Hughes-Davies L, Kouzarides T.** DNA methyltransferase Dnmt1 associates with histone deacetylase activity. *Nat Genet*. 2000;24:88–91.
25. **Fuks F, Burgers WA, Godin N, Kasai M, Kouzarides T.** Dnmt3a binds deacetylases and is recruited by a sequence-specific repressor to silence transcription. *Embo J*. 2001;20:2536–2544.
26. **Dobbing J, Sands J.** Growth and development of the brain and spinal cord of the guinea pig. *Brain Res*. 1970;17:115–123.
27. **Owen D, Matthews SG.** Prenatal glucocorticoid exposure alters hypothalamic-pituitary-adrenal function in juvenile guinea pigs. *J Neuroendocrinol*. 2007;19:172–180.
28. **Dunn E, Kapoor A, Leen J, Matthews SG.** Prenatal synthetic glucocorticoid exposure alters hypothalamic-pituitary-adrenal regulation and pregnancy outcomes in mature female guinea pigs. *J Physiol*. 2010;588:887–899.
29. **Setiawan E, Jackson MF, MacDonald JF, Matthews SG.** Effects of repeated prenatal glucocorticoid exposure on long-term potentiation in the juvenile guinea-pig hippocampus. *J. Physiol*. 2007;581:1033–1042.
30. **Iqbal M, Moisiadis VG, Kostaki A, Matthews SG.** Transgenerational effects of prenatal synthetic glucocorticoids on hypothalamic-pituitary-adrenal function. *Endocrinology*. 2012;153:3295–3307.
31. **Crudo A, Petropoulos S, Moisiadis VG, et al.** Prenatal synthetic glucocorticoid treatment changes DNA methylation States in male organ systems: multigenerational effects. *Endocrinology*. 2012;153:3269–3283.
32. **Weaver IC, Meaney MJ, Szyf M.** Maternal care effects on the hippocampal transcriptome and anxiety-mediated behaviors in the offspring that are reversible in adulthood. *Proc Natl Acad Sci USA*. 2006;103:3480–3485.
33. **Dean F, Matthews SG.** Maternal dexamethasone treatment in late gestation alters glucocorticoid and mineralocorticoid receptor mRNA in the fetal guinea pig brain. *Brain Res*. 1999;846:253–259.
34. **Owen D, Matthews SG.** Repeated maternal glucocorticoid treatment affects activity and hippocampal NMDA receptor expression in juvenile guinea pigs. *J Physiol*. 2007;578:249–257.
35. **Keightley MC, Fuller PJ.** Cortisol resistance and the guinea pig glucocorticoid receptor. *Steroids*. 1995;60:87–92.
36. **Brown SE, Szyf M.** Dynamic epigenetic states of ribosomal RNA promoters during the cell cycle. *Cell Cycle*. 2008;7:382–390.
37. **Crane-Robinson C, Myers FA, Hebbes TR, Clayton AL, Thorne AW.** Chromatin immunoprecipitation assays in acetylation mapping of higher eukaryotes. *Methods Enzymol*. 1999;304:533–547.
38. **Weaver IC, Cervoni N, Champagne FA, et al.** Epigenetic programming by maternal behavior. *Nat Neurosci*. 2004;7:847–854.
39. **Agilent Technologies.** 2010 Agilent Mammalian ChIP-on-chip Protocol.
40. **Team RDC. 2007** R: a language and environment for statistical computing. Vienna, Austria: R Foundation for Statistical Computing.
41. **Bolstad BM, Irizarry RA, Astrand M, Speed TP.** A comparison of normalization methods for high density oligonucleotide array data based on variance and bias. *Bioinformatics*. 2003;19:185–193.
42. **Borghol N, Suderman M, McArdle W, et al.** Associations with early-life socio-economic position in adult DNA methylation. *Int J Epidemiol*. 2012;41:62–74.
43. **Clark SJ, Harrison J, Paul CL, Frommer M.** High sensitivity mapping of methylated cytosines. *Nucleic Acids Res*. 1994;22:2990–2997.
44. **Drake AJ, Raubenheimer PJ, Kerrigan D, McInnes KJ, Seckl JR, Walker BR.** Prenatal dexamethasone programs expression of genes in liver and adipose tissue and increased hepatic lipid accumulation but not obesity on a high-fat diet. *Endocrinology*. 2010;151:1581–1587.
45. **Challis JRG, Matthews SG, Gibb W, Lye SJ.** Endocrine and paracrine regulation of birth at term and preterm. *Endocr Rev*. 2000; 21:514–550.
46. **Thomassin H, Flavin M, Espinas ML, Grange T.** Glucocorticoid-induced DNA demethylation and gene memory during development. *EMBO J*. 2001;20:1974–1983.
47. **Dalle M, Delost P.** Plasma and adrenal cortisol concentrations in foetal, newborn and mother guinea-pigs during the perinatal period. *J Endocrinol*. 1976;70:207–214.
48. **Dy J, Guan H, Sampath-Kumar R, Richardson BS, Yang K.** Placental 11β-hydroxysteroid dehydrogenase type 2 is reduced in pregnancies complicated with idiopathic intrauterine growth restriction: evidence that this is associated with an attenuated ratio of cortisone to cortisol in the umbilical artery. *Placenta*. 2008;29:193–200.
49. **Mark PJ, Augustus S, Lewis JL, Hewitt DP, Waddell BJ.** Changes in the placental glucocorticoid barrier during rat pregnancy: impact on placental corticosterone levels and regulation by progesterone. *Biol Reprod*. 2009;80:1209–1215.
50. **Borzsonyi B, Demendi C, Pajor A, et al.** Gene expression patterns of the 11beta-hydroxysteroid dehydrogenase 2 enzyme in human placenta from intrauterine growth restriction: the role of impaired feto-maternal glucocorticoid metabolism. *Eur J Obstet Gynecol Reprod Biol*. 2012;161:12–17.
51. **Fisher DA, Klein AH.** Thyroid development and disorders of thyroid function in the newborn. *N Engl J Med*. 1981;304:702–712.
52. **De Vries LS, Heckmatt JZ, Burrin JM, Dubowitz LM, Dubowitz V.** Low serum thyroxine concentrations and neural maturation in preterm infants. *Arch Dis Child*. 1986;61:862–866.
53. **Martin CR, Van Marter LJ, Allred EN, Leviton A.** Antenatal glucocorticoids increase early total thyroxine levels in premature infants. *Biol Neonate*. 2005;87:273–280.
54. **Krozowski ZS, Funder JW.** Renal mineralocorticoid receptors and hippocampal corticosterone-binding species have identical intrinsic steroid specificity. *Proc Natl Acad Sci USA*. 1983;80:6056–6060.
55. **Kliewer SA, Lehmann JM, Milburn MV, Willson TM.** The PPARs and PXRs: nuclear xenobiotic receptors that define novel hormone signaling pathways. *Recent Prog Horm Res*. 1999;54:345–367; discussion 367–348.
56. **Langdown ML, Smith ND, Sugden MC, Holness MJ.** Excessive glucocorticoid exposure during late intrauterine development modulates the expression of cardiac uncoupling proteins in adult hypertensive male offspring. *Pflugers Arch*. 2001;442:248–255.
57. **Bian X, Seidler FJ, Slotkin TA.** Fetal dexamethasone exposure interferes with establishment of cardiac noradrenergic innervation and sympathetic activity. *Teratology*. 1993;47:109–117.
58. **Bian XP, Seidler FJ, Slotkin TA.** Promotional role for glucocorticoids in the development of intracellular signalling: enhanced cardiac and renal adenylate cyclase reactivity to beta-adrenergic and non-adrenergic stimuli after low-dose fetal dexamethasone exposure. *J Dev Physiol*. 1992;17:289–297.
59. **Koenen SV, Mecenas CA, Smith GS, Jenkins S, Nathanielsz PW.** Effects of maternal betamethasone administration on fetal and maternal blood pressure and heart rate in the baboon at 0.7 of gestation. *Am J Obstet Gynecol*. 2002;186:812–817.
60. **Langdown ML, Holness MJ, Sugden MC.** Early growth retardation induced by excessive exposure to glucocorticoids in utero selectively increases cardiac GLUT1 protein expression and Akt/protein kinase B activity in adulthood. *J Endocrinol*. 2001;169:11–22.
61. **Sugden MC, Langdown ML, Munns MJ, Holness MJ.** Maternal glucocorticoid treatment modulates placental leptin and leptin receptor expression and materno-fetal leptin physiology during late pregnancy, and elicits hypertension associated with hyperleptinaemia in the early-growth-retarded adult offspring. *Eur J Endocrinol*. 2001;145:529–539.
62. **Matthews SG.** Antenatal glucocorticoids and programming of the developing CNS. *Pediatr Res*. 2000;47:291–300.
63. **Meaney MJ, Diorio J, Francis D, et al.** Early environmental regulation of forebrain glucocorticoid receptor gene expression: implications for adrenocortical responses to stress. *Dev Neurosci*. 1996;18:49–72.
64. **Truss M, Beato M.** Steroid hormone receptors: interaction with deoxyribonucleic acid and transcription factors. *Endocr Rev*. 1993; 14:459–479.
65. **Kassel O, Herrlich P.** Crosstalk between the glucocorticoid receptor and other transcription factors: molecular aspects. *Mol Cell Endocrinol*. 2007;275:13–29.